Farklı Geometrik Konfigürasyonlara Sahip Silindir Oluklu Sandviç Yapıların Basma Mukavemetlerinin ve Enerji Emiliminin İncelenmesi

Ilyas Bozkurt[1*] iD

[1]Makine Mühendisliği, Mühendislik ve Mimarlık Fakültesi, Muş Alparslan Üniversitesi, Muş, Türkiye.
[1]i.bozkurt@alparslan.edu.tr

Öz

Bu çalışmanın amacı beş farklı geometrik konfigürasyona sahip CFRP kompozit silindir sandviç yapıların basma mukavemetlerini ve enerji absorbelerini sayısal olarak incelemek ve birbirleri ile mukayese etmektir. Çalışmada farklı çekirdek yapıları için kompozit sandviçlerin ezilme performansları (Maksimum ezilme kuvveti (PCF), ortalama ezilme kuvveti (MCF), Ezilme kuvveti verimliliği (CFE), enerji emilimi (EA) ve spesifik enerji emilimi (SEA)) ve meydana gelen hasar türleri belirlenmiş. Basma analizleri *LS DYNA* sonlu elemanlar programında *MAT-54* malzeme modeli kullanılarak *Hashin hasar kriteri*, *Kohezif Bölge Modeli (CZM)* ve *Bilinear traction-separation* yasasının kombinasyonuna dayalı ilerlemeli hasar analizi ile gerçekleştirilmiştir. Çalışmada beş farklı numune arasında PCF değeri en yüksek eksenel oluklu çekirdek yapılı Trapeozidal olurken en düşük ise dairesel oluklu çekirdek yapılı Arc shaped olmuştur. Eksenel arc shaped SEA değeri en yüksek sandviç yapı olurken, dairesel sinusoidal oluklu çekirdek ise SEA değeri en düşük sandviç yapı olmuştur. Eksenel ve dairesel oluklu çekirdek arasında sinusoidal yapının CFE değeri en yüksek olarak belirlenmiştir. Sandviç yapıların deformasyon davranışlarına çekirdek yapısının etkisinin yüksek olduğu görülmüştür.

Anahtar kelimeler: Dairesel sandviç kompozit, Basma testi, Ezilme dayanımı, İlerlemeli hasar analizi, Sonlu elemanlar yöntemi

---

*Yazışılan yazar

Firat University Journal of Experimental and Computational Engineering

Investigation of Compressive Strength and Energy Absorption of Cylinder Corrugated Sandwich Structures with Different Geometric Configurations

Ilyas Bozkurt[1] *

[1]Department of Mechanical Engineering, Architecture and Engineering Faculty, Mus Alparslan University, Muş, Türkiye.
[1]i.bozkurt@alparslan.edu.tr

Abstract

The aim of this study is to numerically investigate and compare the compressive strength and energy absorption of CFRP composite cylinder sandwich structures with five different geometric configurations. The crushing performances (Peak crushing force (PCF), Mean crushing force (MCF), Crushing force efficiency (CFE), energy absorption (EA) and specific energy absorption (SEA)) of the composite cylinder for different core configurations and the failure types were determined. Compression analyses were performed in *LS DYNA* finite element program using MAT-54 material model with progressive failure analysis based on the combination of Hashin failure criterion, Cohesive Zone Model (CZM) and Bilinear traction-separation law. Among the five different specimens in the study, the highest PCF value was Trapeozidal with axial corrugated core while the lowest was Arc shaped with circular core. Axial arc shaped core was the sandwich structure with the highest SEA value, while circular sinusoidal corrugated core was the sandwich structure with the lowest SEA value. Between axial core and circular core, the CFE value of the sinusoidal core specimen was determined to be the highest. It was observed that the effect of core structure on the deformation behavior of sandwich structures was high.

Keywords: Circular sandwich composite, Compression test, Crashworthiness, Progressive failure analysis, Finite element method

---

*Corresponding author

1. Introduction

Sandwich composite structures with high strength/weight and high energy absorption capacity are actively used in many sectors, especially in the aerospace industry [1]. Sandwich structures are indispensable structures for engineers, especially in components and sections with high energy absorption requirements. Sandwich structures are generally composed of a part called core, which is placed between the upper and lower facesheets [2]. Although the facesheets are usually in the form of plates, different configurations are used in the core structure. Especially with the development of manufacturing technology and production techniques, many different core structures have been produced and their strength values have been studied by researchers. Different types of adhesives such as epoxy or Araldite are used to join the facesheets to the core [3, 4]. Sandwich structures can be produced as flat plates or cylinders depending on the area of use [5]. There is a great need especially in areas where cylindrical structures are used, such as airplane parts, wing sections and bicycle bodies, where lightness and high strength come to the fore.

The main purpose of using corrugated structures in sandwich structures is to reduce the total mass. Even if they are not as light as thin lattice structures, these structures with high strength values can have the strength values required by engineers. If instead of using a corrugated structure, only a hollow and shapeless body was used, it would not be preferred much due to its high weight. It is also known that weight has a great impact on fuel consumption. By using lighter structures, environmental failure can also be minimized. However, since the strength effect also changes with the change of core type, it is an area that can be intervened and controlled for researchers [6-8]. In addition, the effects of strength values of different composite types (such as glass fiber, carbon fiber, kevlar) or alloy types (such as aluminum, steel) can be examined [9].

Many studies have been conducted to improve the strength performance of corrugated sandwich composite structures [2, 10-17]. Zhang et al. [18] investigated the compression performance and failure modes of square honeycomb core sandwich cylinders by experimental measurement, analytical modeling and numerical simulation. Wu et al. [19] investigated four possible failure modes (Euler buckling, axisymmetric buckling, local buckling and face panel crushing of the sandwich cylinders) and their corresponding strength values under compression loading of low density pyramid lattice core sandwich cylinders made of plain woven carbon fiber fabrics. Ge et al. [20] experimentally and numerically investigated the compression behavior and failure modes of a new sandwich structure with bidirectional corrugated cores produced by 3D printing. The study shows that corrugated buckling and fracture are the main failure modes in flat compression. However, the front panels mostly support the loading in the edge direction and no significant deformation is observed. Zhu et al. [21] experimentally, numerically and analytically investigated the axial compression behavior of trapezoidal staggered corrugated truss, bidirectional corrugated truss and hexagonal honeycomb core sandwich plates. Zhu et al. [22] experimentally and numerically investigated the axial and lateral compression behaviors and failure modes of inner square tube, corrugated core and outer square tube produced by hot pressing method. Chen et al. [23] experimentally and numerically performed compression tests to determine the failure modes of the number and core configurations (regular, perpendicular and symmetrical) of multilayer corrugated sandwich panels produced by hot pressing. Han et al. [24] investigated the compression behavior of honeycomb corrugated hybrid core aluminum sandwich structures both experimentally and theoretically.

In this study, unlike the literature, compressive strength values (Peak crushing force (PCF), Mean crushing force (MCF), Crushing force efficiency (CFE), energy absorption (EA) and specific energy absorption (SEA)) and failures of five different cylindrical corrugated sandwich carbon composite structures (Trapezoidal, Rectangular, Arc-shaped, Triangular and Sinusoidal) were determined numerically and compared with each other. Compression simulations were performed in *LS DYNA* finite element program using MAT-54 material model based on *Hashin failure criterion*, *Cohesive Zone Model* (CZM) *and Bilinear traction-separation laws.*

2. Numerical Study

2.1. Finite element model

The compression behavior of carbon fiber cylindrical composite sandwich structures with different core configurations was investigated using the *LS DYNA* finite element program [25]. The solution methodology of the program includes material cards that provide failure models based on the continuous failure mechanism (CDM) [26]. By using models based on CDM, it is possible to see structural failure in a progressive manner. When creating the numerical model, it is important that all specimens are under the same limit and under the same standards. Because in this study, no experimental study was taken as a reference, only the compression behaviors were compared with each other. Therefore, it is important that all specimens are under the same conditions.

In order to determine and compare the compressive strength and energy absorption capabilities of sandwich composite structures, it is necessary to determine crashworthiness parameters. These parameters are calculated from force-displacement curves. Figure 1 shows an example force-displacement curve obtained from a compression test. During the crushing behavior of cylindrical sandwich structures, there are three distinct stages. First stage, plateau stage and densification stage. In the first stage, the crushing force increases rapidly with the crushing distance until it reaches the initial peak force (PCF). This is followed by the plateau stage, characterized by the development of folds in the tubes, causing fluctuations in the crushing force. This fluctuation is caused by the buckling, bending and collapse of the cell walls. Finally, in the densification stage, the crushing force experiences a significant increase due to densification.
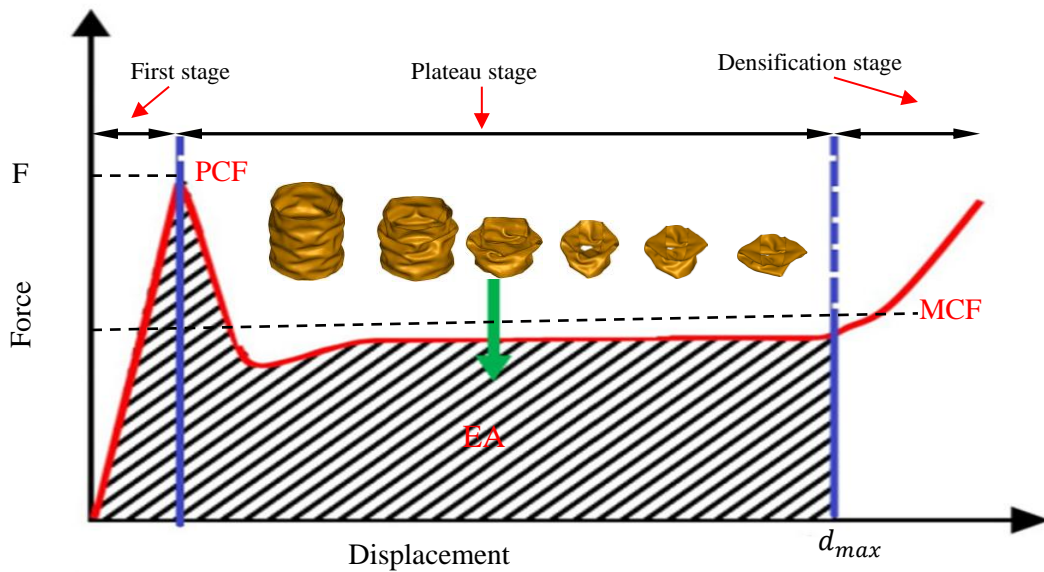
Figure 1. Example force-displacement curve obtained from compression testing

Here, the area under the graph gives the absorption energy (EA) or total inner energy (TIE) (1).

$$EA(dx) = \int_0^{d_x} F(x)dx \tag{1}$$

where d_x is the crush distance and F(x) is the crush force as a function of the crush distance of x.

$$SEA = \frac{EA}{m} \tag{2}$$

Energy per unit of mass is denoted by SEA, where m is mass.

Crushing force efficiency (CFE) represents the ratio of mean crushing force (F mean) to peak crushing force (PCF) and is defined as:

$$CFE = \frac{MCF}{PCF}$$

(3)

Peak breaking force (PCF) is the maximum force value of the system. Mean crushing force (MCF) is considered as the average force.
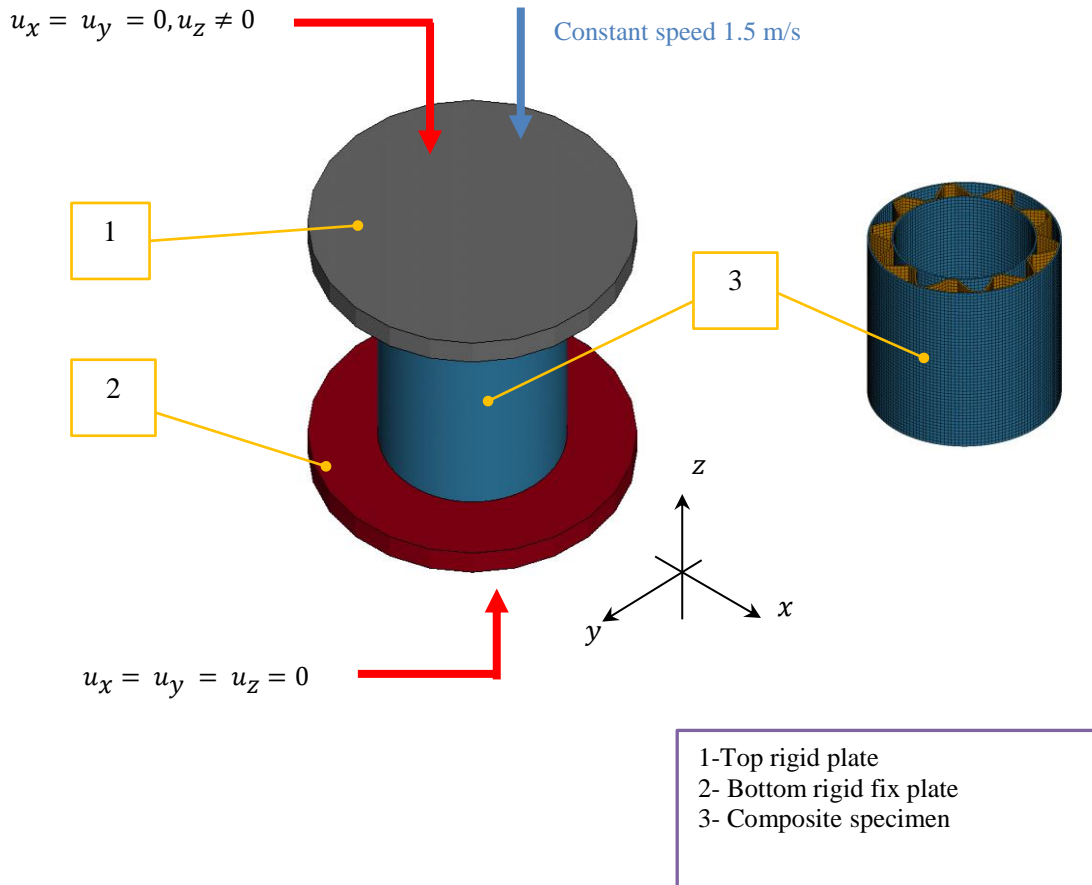

Figure 2. FEM model

In the study, the element mesh size was taken as 2 mm x 2 mm considering the analysis time, efficiency, specimen thickness and 8-node brick solid element (*ELFORM1*) was used as the element type. It is the most commonly used element type as a solid model in the literature [27]. Figure 2 shows the compression test finite element model of cylindrical sandwich composites. The specimens are placed between the upper and lower rigid plates. The lower plate motions were kept constant in the x, y and z directions, while the upper plate was allowed to move freely in the z direction. The compression speed of the top plate was set as 1.5 m/s considering the processing time and efficiency. "CONTACT_AUTOMATIC_SURFACE_TO_SURFACE" contact card was defined between the top plate and the composite. 'CONTACT_AUTOMATIC_SINGLE_SURFACE' contact card was used to prevent interference between the elements in the composite specimens.

Both dynamic and static friction coefficients were defined as 0.2 [27]. For the quasi-static compression test of the composite specimens, the upper plate was moved in the *z* direction using the BOUNDARY_PRESCRIBED_MOTION_ SET card. The bottom plate was assigned as fixed. To avoid dynamic effect, the initial speed was increased linearly starting from 0 up to 1.5 m/s and then kept constant. Different core structures shown in Figure 3 were used in the study. The diameter x length dimensions of the axial corrugated core specimens are 100 mm x 100 mm while the circular core specimens are 115 mm x 140 mm. The unit cell dimensions and weights of these core structures are given in Table 1. Cell widths and cell heights are the same. In order to make their weights the same, it was tried to equalize their weights by reducing the material thickness and entering their densities in the finite element program. The maximum difference between the weights is 1.65%. Therefore, a healthy comparison can be made under the same boundary conditions by considering the cell width, cell height and weights equal. From each figure given in Table 1, two different corrugated core structures, axial and circular, were formed by bending. It is shown in Figure 4 in stages. The specimens used in the study and the pictures of the core structures are given in Table 2.
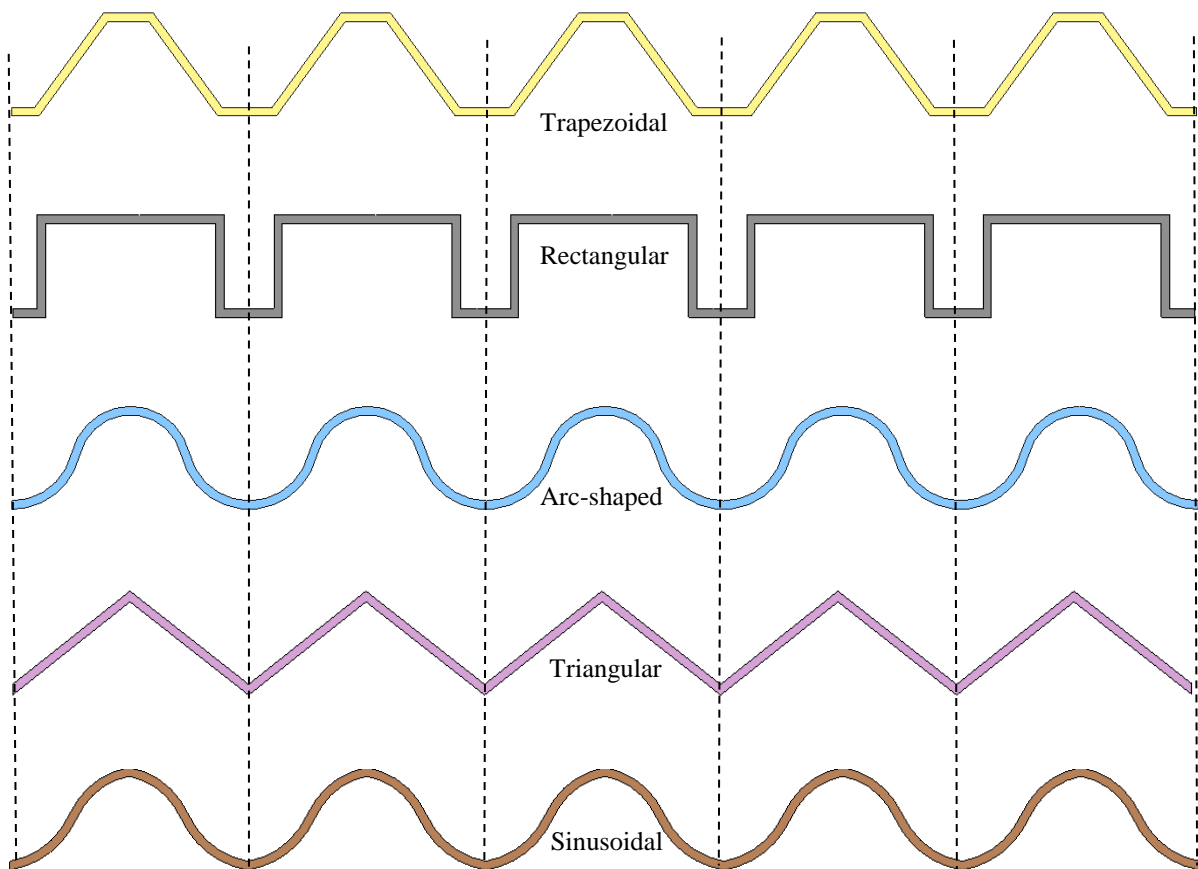
Figure 3. Different corrugated core structures used in the research

Table 1. Dimensions and masses of corrugated core structures

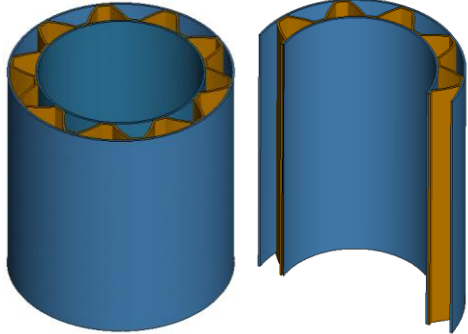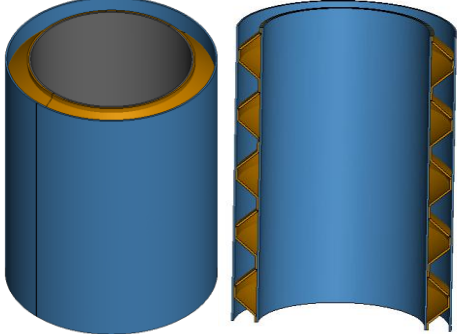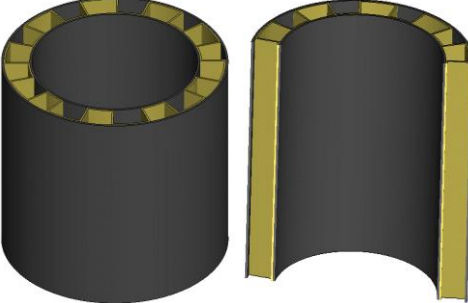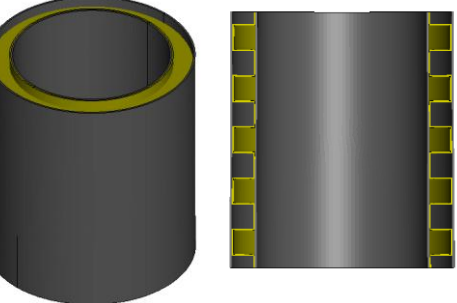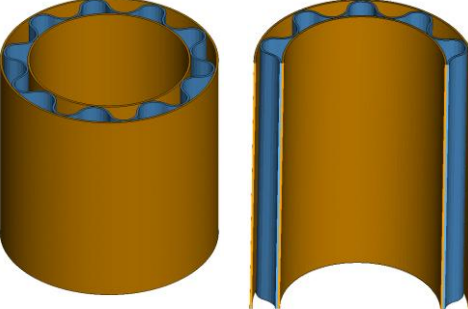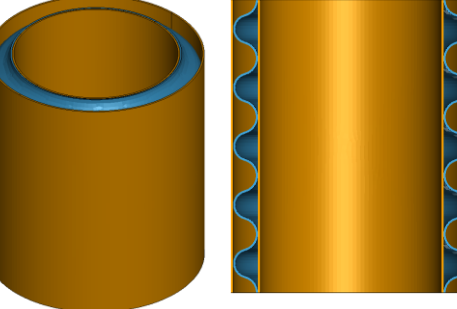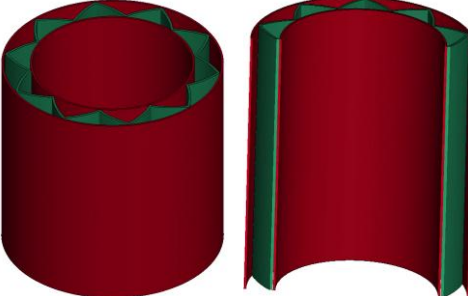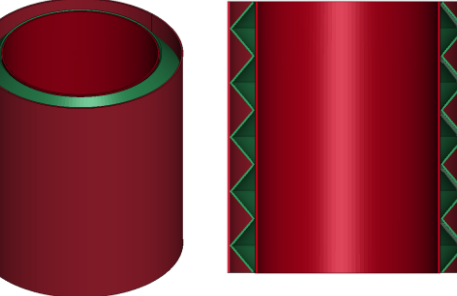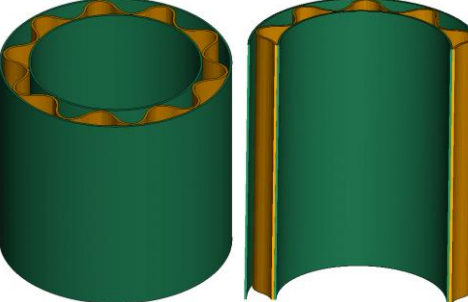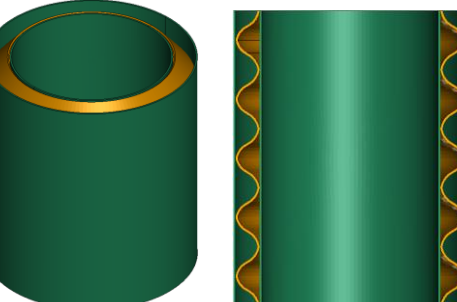| Cell name	Cell Shape	Axial Mass (gr)	Circular Mass(gr)
Trapezoidal		145.778	231.931
Rectangular		145.879	220.000
Arc-shaped		144.997	230.559
Triangular		146.666	223.775
Sinusoidal		147.394	223.775

Axial corrugated core

Circular corrugated core
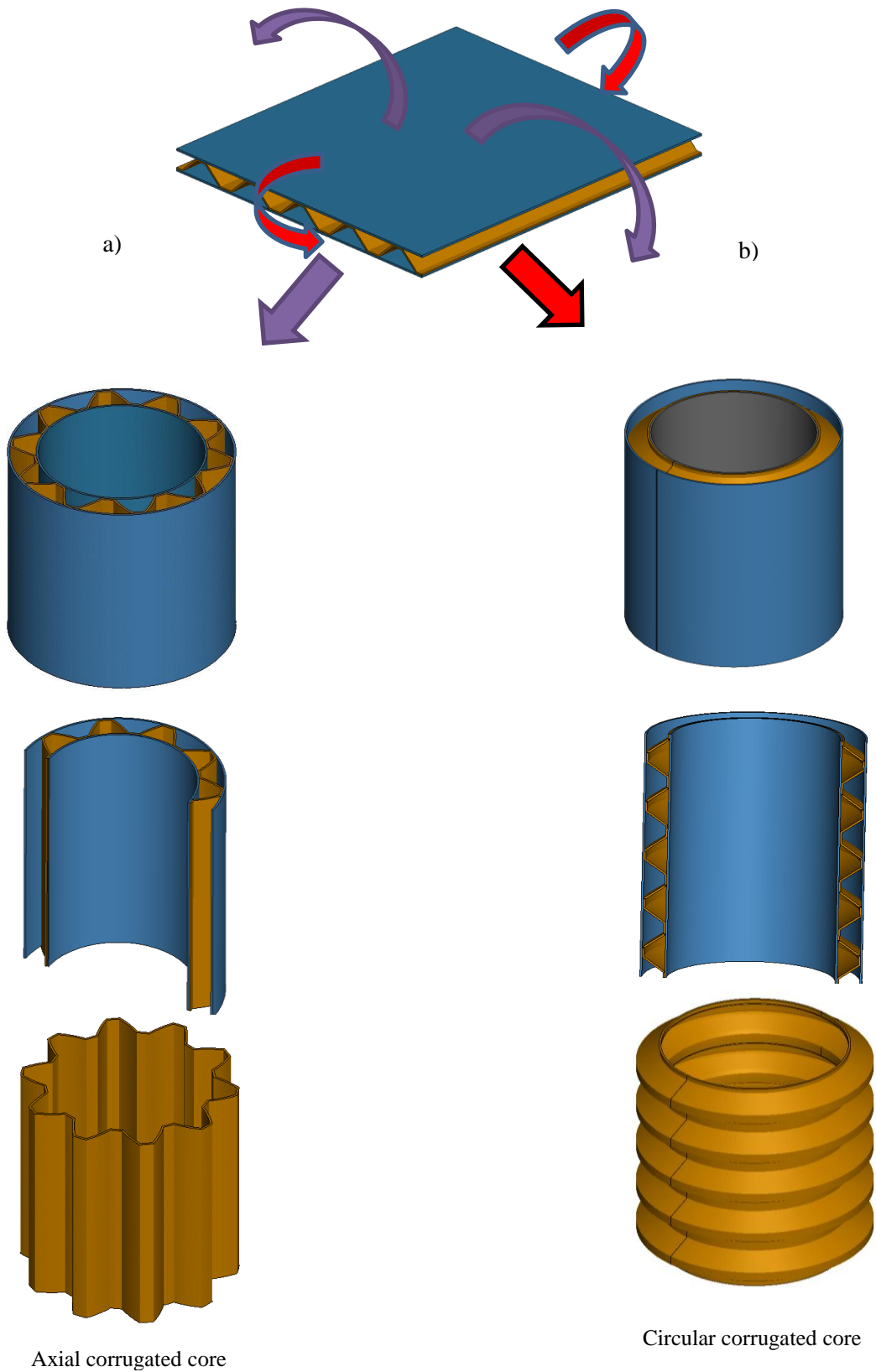
Figure 4. Specimens (a) axial corrugated core, (b) circular corrugated core

Table 2. Compression specimens

Specimens	Axial corrugated core	Circular corrugated core
Trapezoidal		
Rectangular		
Arc-shaped		
Triangular		
Sinusoidal		

2.2. Material models

It is very important to determine the material model in *LS DYNA* finite elements. Because the strength values and failure deformations in the structure exposed to load are realized according to the determined criterion. There are many material models to define the composite structure in *LS DYNA*. Among these, the most widely used material models by researchers are *MAT 22, MAT 54/55, MAT 58, MAT 59* and *MAT 162*. The main difference between these material models is the failure criterion and material behavior as a result of loading. Strength parameters (transverse compressive strength, longitudinal compressive strength, transverse tensile strength and shear strength) are used to determine the failure to the material. is needed. Among these material models, the *MAT-22* material model based on the Hashin failure criterion, which is the most widely used in the literature, was used in the study. When defining the *MAT54* material model, 25 input values are needed. Of these, 15 parameters are material constants given in Table 3. The remaining 10 numerical parameters (shown in Table 4) are obtained by calibrating through finite elements [28].

Table 3. Mechanical parameters of the CFRP composite [27]

Symbol	Property	Value	Unit
ρ	Density	1500	kg/m^3
E_a, E_b	Young modulus a and b direction	43.7	GPa
E_c	Young modulus in c direction	15	GPa
v_{ab}	Poisson's ratio in ab plane	0.21	-
v_{bc}	Poisson's ratio in bc plane	0.21	-
v_{ca}	Poisson's ratio in ca plane	0.21	-
G_{ab}	Shear modulus in ab plane	14.18	GPa
G_{bc}	Shear modulus in bc plane	14.65	GPa
G_{ca}	Shear modulus in ca plane	14.65	GPa
S_{aT}	Tensile strength a direction	0.589	GPa
S_{aC}	Compressive strength a direction	0.1096	GPa
S_{bT}	Tensile strength b direction	0.589	GPa
S_{bC}	Compressive strength b direction	0.1096	GPa
S_{ab}	Shear strength in ab plane	0.1082	GPa

Table 4. Failure parameters of the CFRP composite.

Symbol	Description	Unit
DFAILM	Transverse matrix failure strain experimental	0.0
DFAILS	Shear failure strain experimental	0.0
DFAILT	Tensile fiber failure strain experimental	0.0
DFAILC	Compressive fiber failure strain experimental	0.0
TFAIL	Timestep for element deletion computational	0.16
Alpha	Shear stress parameter failure dependent	0.0
Soft	Strength reduction factor failure dependent	0.7
FBRT	Reduction factor for X_t failure dependent	1
YCFAC	Reduction factor for X_c failure dependent	3
EFS	Efective failure strain computational	0.90

2.3. Modeling of adhesive layer

In sandwich structures, the core structure and the upper and lower facesheets structures need to be bonded to each other. Different types of adhesives such as resin or Araldite 55 are used to ensure this bonding. These adhesives are applied to the contact points of the core and facesheet structures and adhesion is achieved by waiting for a certain period of time at room temperature. This adhesion is of great importance in absorbing the force coming to the upper facesheet in case of impact and distributing it homogeneously to other areas. Therefore, this adhesion and separation due to impact is based on some mechanical principles. In the literature, it is characterized as CZM with a bilinear traction-separation law. This law is based on the application of 3 independent parameters. The traction t_0, between the layers when the force is applied, the separation distance δ_0 when the failure starts and the G_C under this curve. After the impact occurs, the separation between the layers occurs according to this principle (Figure 5).
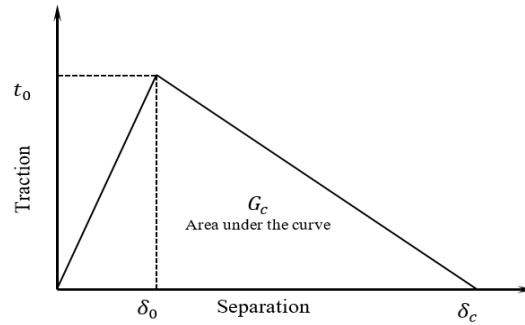

Figure 5. Bilinear traction-separation law

The connection between the core and the facesheet can be achieved in two ways in FEM. First, it can be achieved by assigning a thin film material here. Or instead, this adhesion can be achieved by providing a connection between the surfaces. Dogan et al [29] determined that this method is effective instead of using intermediate material. In this study, The CONTACT_AUTOMATIC SURFACE TO SURFACE TIEBREAK contact card was used to bond the top and bottom cover to the core material in between. While adhesion is achieved here, separations occur based on the Bilinear traction-separation law. With this contact card, the nodes making contact in the beginning connect with each other according to the following criterion.

$$\left(\frac{|\sigma_n|}{NFLS}\right)^2 + \left(\frac{|\sigma_s|}{SFLS}\right)^2 \geq 1 \tag{5}$$

Here, while σ_n and σ_s are the current normal and shear stresses, *NFLS* and *SFLS* are respectively the interface and shear strength. When the condition of Equation (5) is met, interface node stress is decreased to zero and the connection between the nodes is released. The contact parameters for Araldite 2015, which was used as the adhesive material in this research, are provided in Table 5.

Table 5. Cohesive parameters between core and face sheets interfaces [30]

Contact Tiebreak Variable	Description	Value	Units
NFLS	Peak traction in normal direction	21.63×10^9	Pa
SFLS	Peak traction in tangential direction	17.9×10^9	Pa
PARAM	Exponent of mixed-mode criteria	1	-
ERATEN	Energy release rate for Mode I	430	N/m
ERATES	Energy release rate for Mode II	4700	N/m
CT2CN	Ratio of tangential stiffness to normal stiffness	1	-
CN	Normal stiffness	8080	Pa/m

2.4. MAT_54-55: Enhanced composite failure model

It is the most widely used material model in the analysis of composite structures. In the material model, it is assumed that the material is orthotropic and linear elastic in the absence of any failure. In this model, *MAT 54* failure criterion was proposed by *Chang* and *MAT 55* failure criterion was proposed by *Tsai-Wu*. The operating principle of this material model is the same as that of *MAT 22*, but additionally includes a compression failure mode. The *Chang–Chang criterion* (*MAT -54*) is given below [27];
Tensile fibre ($\sigma_{11} > 0$).

$$\left(\frac{\sigma_{11}}{S_1}\right)^2 + \bar{\tau} = 1 \tag{6}$$

All moduli and Poisson's ratios are set to zero when the tensile fibre failure criteria are met, that is $E_1 = E_2 = G_{12} = \upsilon_{12} = \upsilon_{21} = 0$ All the stresses in the elements are reduced to zero, and the element layer has failed.
Failure mode for compressive fibre ($\sigma_{11} > 0$),

$$\left(\frac{\sigma_{11}}{S_{12}}\right)^2 = 1 \tag{7}$$

Failure mode for tensile matrix ($\sigma_{11} > 0$),

$$\left(\frac{\sigma_{22}}{S_2}\right)^2 + \bar{\tau} = 1 \tag{8}$$

Failure mode for compressive matrix

$$\left(\frac{\sigma_{22}}{2S_{12}}\right)^2 + \left[\left(\frac{C_2}{2S_{12}}\right) - 1\right]\frac{\sigma_{22}}{C_2} + \bar{\tau} = 1 \tag{9}$$

Where E_1 and E_2 are the longitudinal and transverse elastic moduli, respectively, G_{12} is the shear modulus, υ_{12} and υ_{21} are the in-plane Poisson's ratios.

3. Results and Discussion

The force-displacement plots of axial corrugated core and circular corrugated core cylindrical sandwich composite structures under axial load are shown in Figure 6a and 6b respectively. Figure 6a shows the graphs of five different axial corrugated core structures as well as the without core specimen after compression test. The PCF value for the without core specimen is 24.5 kN while the MCF value is 4.22 kN. Core was added to this without core specimen in five different configurations and compression simulations were performed again. The aim here is to increase the crashworthiness performance without increasing the weight too much. When the graphs are analyzed, the load for all specimens increased to the maximum point and then decreased [27]. It is seen that the specimen with the highest PCF value is the specimen with Trapeozidal core.
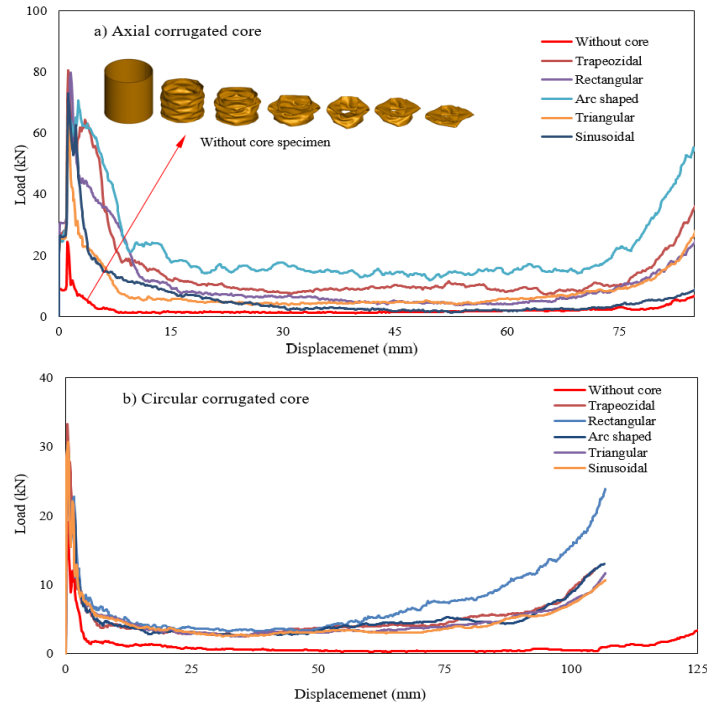
Figure 6. Force-displacement results for a) Axial corrugated core and

It was observed for all specimens that the force value increased to the maximum point, the force decreased slightly and then increased again. The reason for this is that fluctuations occur on the structure due to the load. After the load drop, the force value continued at a certain value until the end of the crushing test [31]. This value is obtained in parallel with the MCF value. According to this, it is seen that the MCF value of the specimen with Arc shaped core structure is higher than the others. This is because these force values are averaged when determining the average force value. Since densification occurred in the material structure due to the effect of crushing force in the last section, the load value increased [32].

Figure 6b shows the graphs of five different circular corrugated core structures and without core specimen after compression test. The PCF value for the without core specimen is 19.11 kN while the MCF value is 1 kN. When the graph is analyzed, it is seen that the force reached the maximum point and then the force value decreased sharply. Then, it was observed that crushing occurred at an average force value. In the last section, it was determined that an increase in the load value occurred due to the densification situation. It is noticed that the last part of the Without core specimen has a later densification effect unlike the other specimens. The reason for this is the absence of core structure and the amount of material for densification is less than the other specimens.

Figure 7 shows the PCF and EA results for sandwich composites with axial and circular corrugated core structure after compression test. When the PCF values are examined in Figure 7a, the maximum peak load value was obtained in the axial corrugated core Trapeozidal specimen with 80.53 kN. The minimum was 26.69 kN for the Arc shaped specimen. Accordingly, the PCF value for the axial corrugated core increased by a maximum of 2.28 times compared to the without core specimen. When the maximum PCF value obtained from the circular corrugated core specimen is compared with the without core specimen, an increase of 0.74 times is observed. When the EA values are analyzed in Figure 7b, the maximum EA value among all specimens was obtained as 1626.2 J for the axial corrugated Arc shaped core specimen. The minimum value occurred in the circular sinusoidal specimen with 452 J. When the energy absorption values of with core and without core specimens are compared, the maximum value is increased 3.82 times for axial core structures and 5.71 times for circular core.
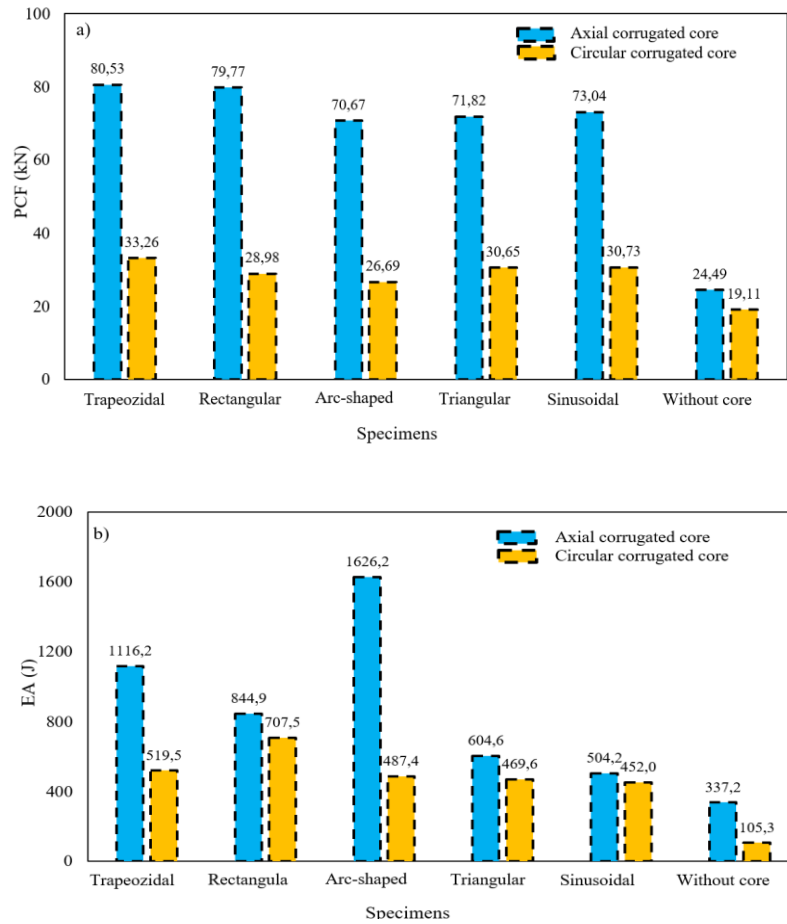
Figure 7. a) PCF and b) EA results

Although the EA value increases by using circular core, the maximum value remains low when compared to axial core. But what is important here is the SEA value. That is, the energy absorbed per weight. The results regarding this will be given in the following section.

At the end of the compression test, many results are obtained about the mechanical structure and strength of the material. These results provide vital information about the structure and provide researchers with important information about the behavior of the structure under load and its strength limits [33]. The PCF value is an important parameter for assessing crashworthiness [6]. But the most important parameter affecting the energy absorption capacity is MCF. Because the energy absorption value is calculated from the area under the MCF. In some cases, the PCF value may be too high while the MCF value may be too low. Therefore, the higher the MCF value, the higher the energy absorption capacity. Here the CFE value expresses the efficiency between these two. It should be as high as possible to control the energy absorption efficiency without any failure during an accident [34]. Figure 8a-c shows the SEA, MCF and CFE results of the specimens at the end of the compression simulation. When the SEA results in Figure 8a are examined, the axial corrugated arc shaped core specimen is the sandwich structure with the highest SEA value with 11.2 J/g, while the circular sinusoidal corrugated core with 2.02 J/g is the lowest sandwich structure. By using axial corrugated core structure, the maximum SEA value increased by 65% compared to without core structure. By using circular corrugated core structure, the maximum SEA value increased by 136.7% compared to without core structure. When the MCF results are analyzed in Figure 8b, the MCF value of the axial corrugated arc shaped core specimen is the highest with 20.33 kN, while the circular sinusoidal specimen has the lowest value with 4.3 kN. Already in Figure 6, these results are clearly seen in the graphs. Figure 8c shows the crushing force efficiency (CFE) results. Here, the highest CFE value means that the higher the energy absorption capacity in case of accident or loading. In other words, the
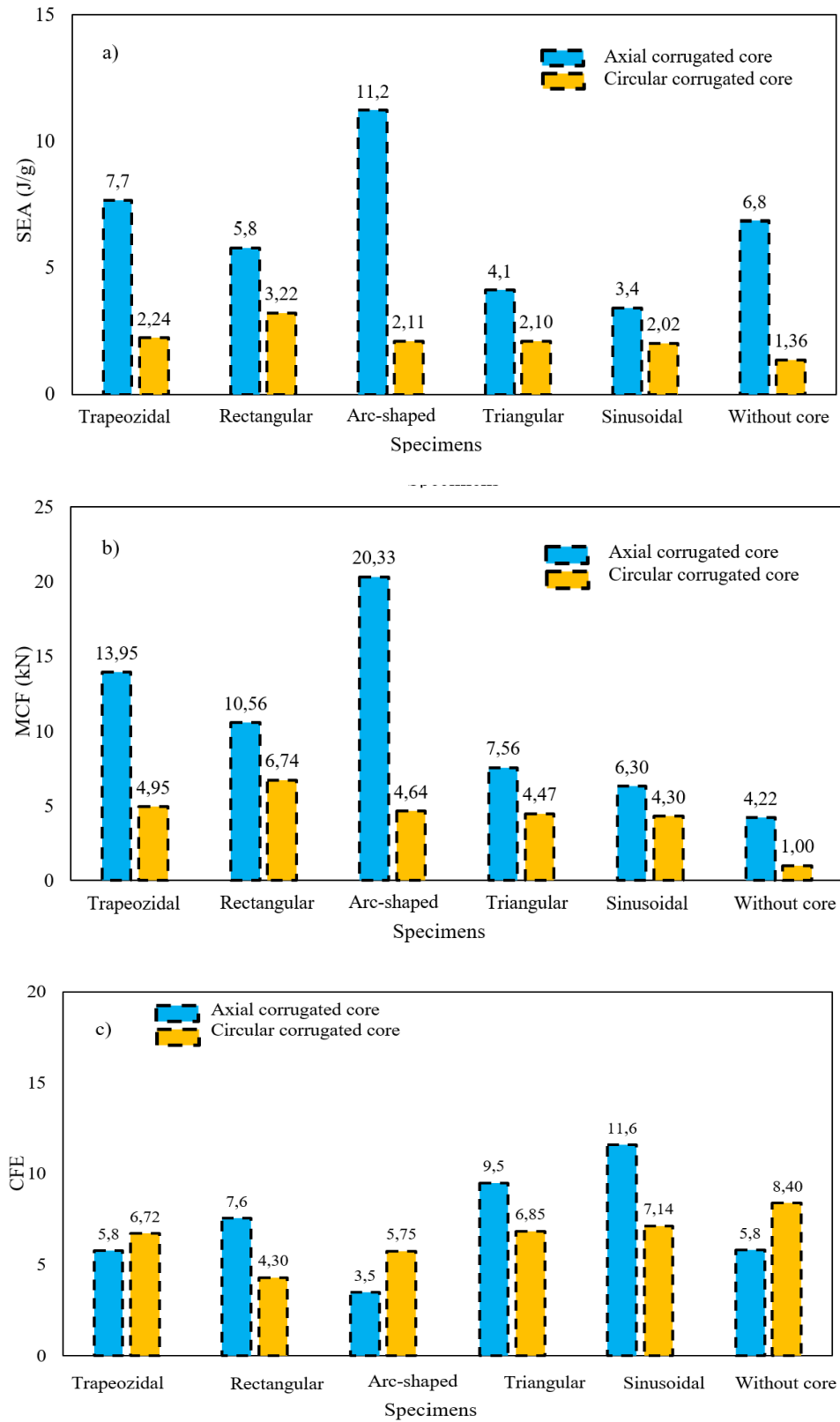
Figure 8. a) SEA and b) MCF and c) CFE results
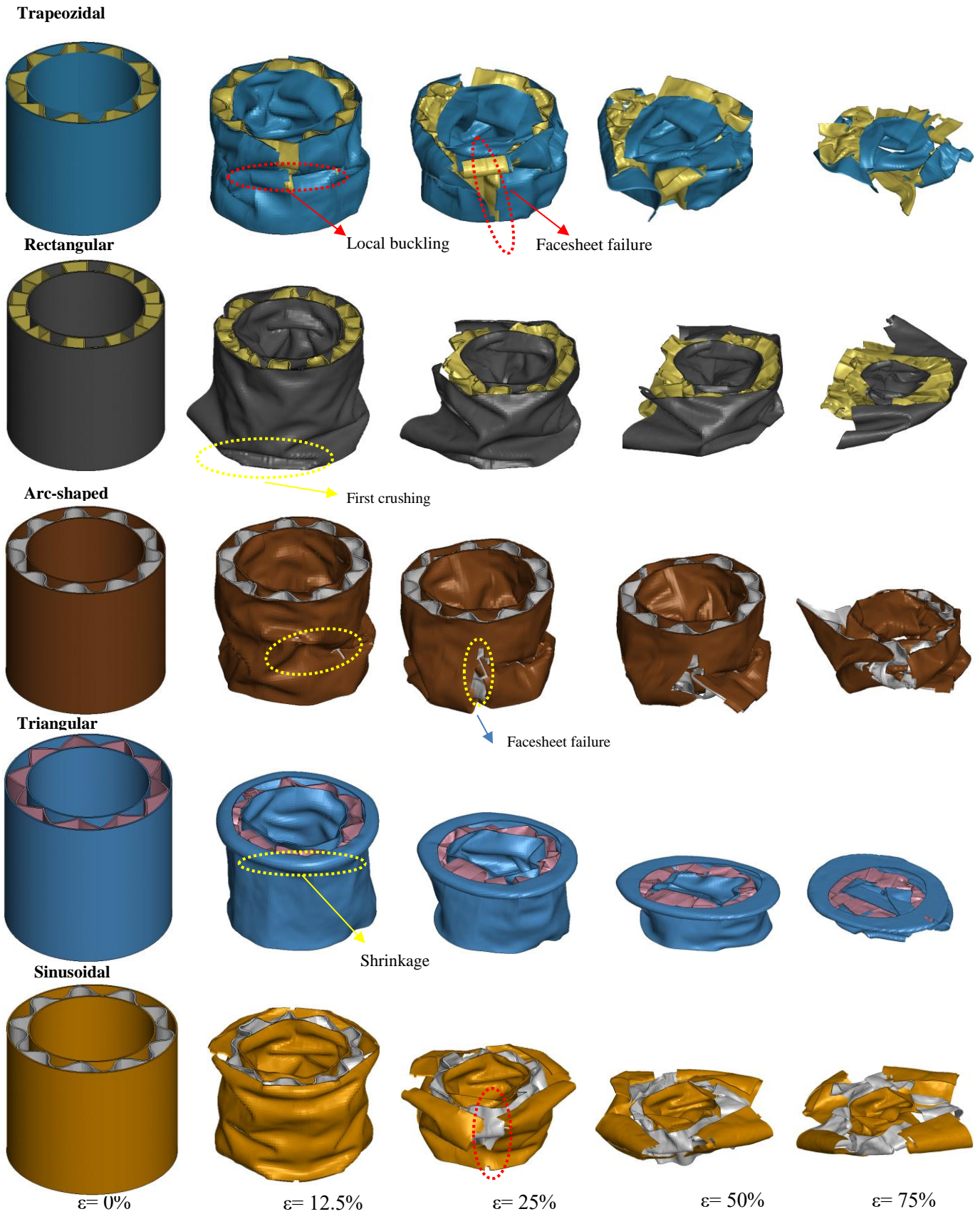
Figure 9. Deformations after compression test for axial corrugated core
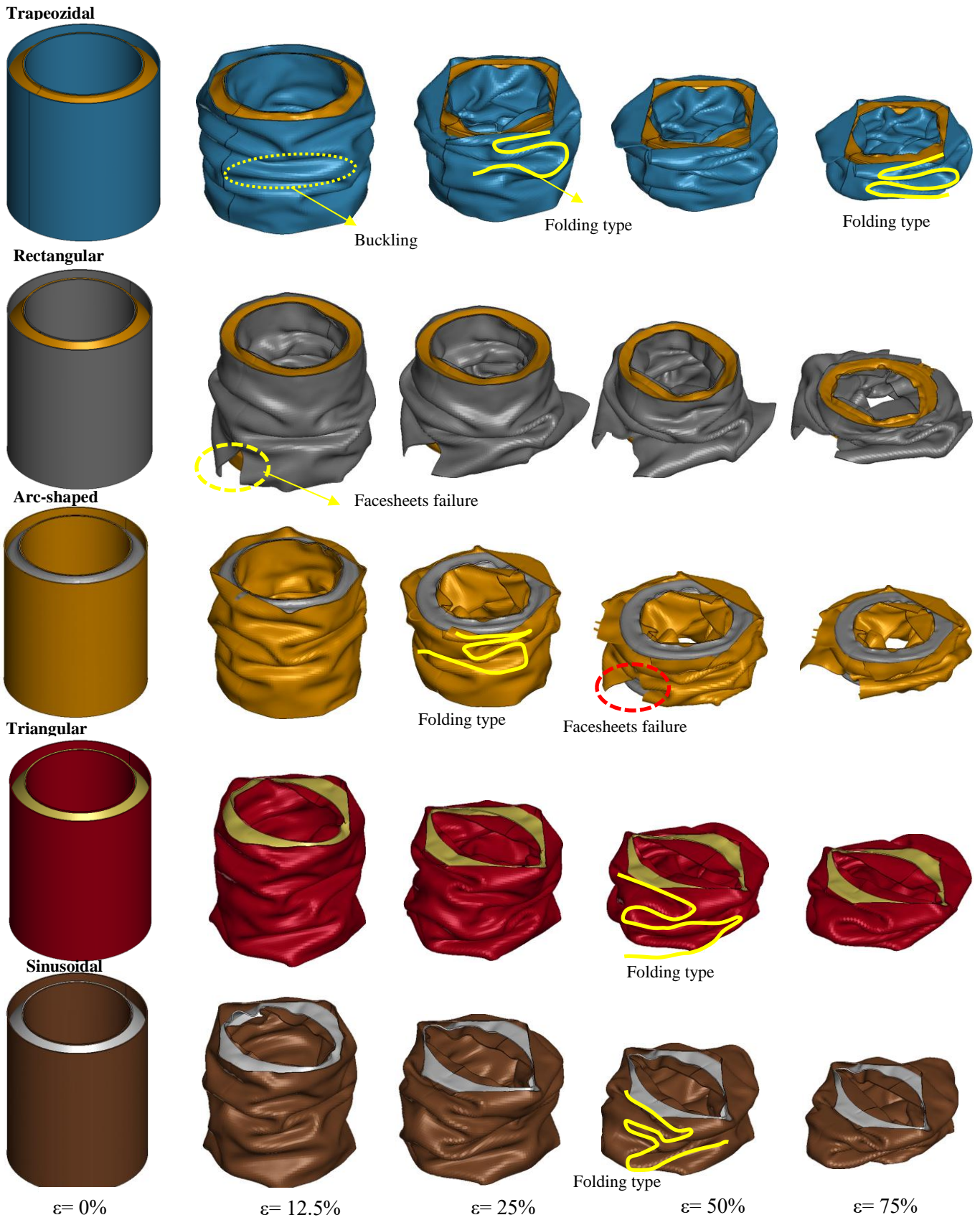
Trapeozidal

Rectangular

Arc-shaped

Triangular

Sinusoidal

ε= 0%   ε= 12.5%   ε= 25%   ε= 50%   ε= 75%

Figure 10. Deformations after compression test for circular corrugated core

CFE value is always the highest value, which is a desired result for researchers working in this field. Among the axial core and circular core specimens, the CFE value of the sinusoidal core specimen was the highest. The lowest was Arc-shaped for Axial core and rectangular core for circular core.

The deformations of axial and circular corrugated sandwich composite structures are given in Figure 9 and Figure 10 respectively. After the load is applied to the sandwich structure, it gradually increases with displacement and no significant deviation in linear behavior is observed until the peak [18]. Here, the structure can resist up to a point while the load increases [35]. Then a sharp drop in load occurs. This is the scenario that generally occurs when any specimen is tested in compression [36]. Depending on the type of specimen used, the peak crushing force value and the average load amount with sudden load drop may vary.

Figure 9 shows the deformations of axial core sandwich structures. Due to the difference in the structural configuration of the five different specimens, the failure types or initial failures are different from each other. In the trapeozidal specimen, buckling failure and facesheet failure were observed in the center of the specimen due to loading. In Rectangular, the first failure started at the base of the specimen, while both buckling and facesheet failure were observed in the arc shaped specimen. In the triangular specimen, the specimen was folded with shrinkage failure, while in the sinusoidal specimen, large deformation occurred in the failure. Figure 10 shows the deformation pictures of circular core sandwich structures. When the post-compression deformations of all specimens were examined, it was seen that the deformation rate was higher in axial core structures. As the compression rate increased, the folding rate also increased. While some specimens showed face sheet failure (rectangular and arc-shaped), most of them were deformed by folding.

4. Conclusions

In this study, the crushing performance of sandwich composite structures with different core configurations (Trapezoidal, Rectangular, Arc-shaped, Triangular and Sinusoidal) under quasi-static compression loading was determined using the finite element method. The numerical model was applied by performing *progressive failure analysis* with *MAT-54* material model in *LS DYNA* finite element model. In the study, the performances (Peak force (PF), Mean crushing force (MCF), Crushing force efficiency (CFE) and specific energy absorption (SAE)) and failure types for different core structures and core orientations (axial-circular) were determined. Based on the data obtained at the end of the study, the results can be summarized as follows:

- Among the five different specimens, the Trapeozidal specimen with axial corrugated core has the highest PCF value while the Arc shaped specimen with circular core has the lowest PCF value. Accordingly, the PCF value for the axial corrugated core increased by a maximum of 2.28 times compared to the without core specimen. The maximum PCF value obtained from the circular corrugated core specimen increased by 0.74 times compared to the without core specimen.
- When the EA values were analyzed, the maximum EA value among all specimens was the axial corrugated Arc shaped specimen, while the minimum value was the circular sinusoidal specimen. When the energy absorption values of with core and without core specimens are compared, the maximum energy absorption value for axial core structures increased by 3.82 times and 5.71 times for circular core.
- Using the axial corrugated core, the energy absorption value increased by a maximum of 3.82 times, while with the circular corrugated core, the energy absorption value increased by a maximum of 5.72 times.
- Axial corrugated arc shaped core specimen was the sandwich structure with the highest SEA value, while circular sinusoidal corrugated core was the sandwich structure with the lowest SEA value. By using the axial corrugated core structure, the maximum SEA value increased by 65% compared to the without core structure. By using circular corrugated core structure, the maximum SEA value increased by 136.7% compared to without core structure.
- The MCF value of the axial corrugated arc shaped core specimen was the highest while the circular sinusoidal specimen had the lowest value. Among the axial core and circular core specimens, the

CFE value of the sinusoidal core specimen was the highest. The lowest value was Arc-shaped for axial core and rectangular core for circular core.
- The deformation behavior of corrugated sandwich structures mainly depends on the core type. Folding shape, bending type, facesheets failure differ according to the core type.
- This numerical research has the potential to make a great contribution to the literature by being supported experimentally in future studies.

Nomenclature

CFE: Crushing force efficiency
CZM: Cohesive Zone Model
EA: Energy absorption
MCF: Mean crushing force
PCF: Peak-crushing force
SEA: Specific energy absorption

5. Author Contribution Declaration

In the study carried out, Author contributed to the formation of the idea, design and literature review, evaluation of the results, procurement of the materials used and examination of the results, and checking the article in terms of spelling and content.

6. Ethics Committee Approval and Conflict of Interest Declaration

There is no need to obtain ethics committee permission for the article prepared. There is no conflict of interest with any person/institution in the prepared article.

7. References

[1] B. Kiyak, and M. O. Kaman, "Mechanical properties of new-manufactured sandwich composite having carbon fiber core," J. Compos. Mater., vol. 53, no. 22, pp. 3093-3109, 2019.

[2] M. O. Kaman, M. Y. Solmaz, and K. Turan, "Experimental and numerical analysis of critical buckling load of honeycomb sandwich panels," J. Compos. Mater., vol. 44, no. 24, pp. 2819-2831, 2010.

[3] M. Albayrak, M. O. Kaman, and I. Bozkurt, "Experimental and Numerical Investigation of the Geometrical Effect on Low Velocity Impact Behavior for Curved Composites with a Rubber Interlayer," Appl. Compos. Mater., vol. 30, no. 2, pp. 507-538, 2023.

[4] M. Albayrak, M. O. Kaman, and I. Bozkurt, "The effect of lamina configuration on low-velocity impact behaviour for glass fiber/rubber curved composites," J. Compos. Mater., vol. 57, no. 11, pp. 1875-1908.

[5] Q. Zheng, D. Jiang, C. Huang, X. Shang, and S. Ju, "Analysis of failure loads and optimal design of composite lattice cylinder under axial compression," Compos. Struct., vol. 131, pp. 885-894, Nov. 2015.

[6] S. Hou, S. Zhao, L. Ren, X. Han, and Q. Li, "Crashworthiness optimization of corrugated sandwich panels," Mater. Des., vol. 51, pp. 1071-1084, 2013.

[7] Y. Hu, W. Li, X. An, and H. Fan, "Fabrication and mechanical behaviors of corrugated lattice truss composite sandwich panels," Compos. Sci. Technol., vol. 125, pp. 114-122, 2016.

[8] W. He, J. Liu, S. Wang, and D. Xie, "Low-velocity impact response and post-impact flexural behaviour of composite sandwich structures with corrugated cores," Compos. Struct., vol. 189, pp. 37-53, Apr. 2018.

[9] J. Liu, W. He, D. Xie, and B. Tao, "The effect of impactor shape on the low-velocity impact behavior of hybrid corrugated core sandwich structures," Compos. B Eng., vol. 111, pp. 315-331, 2017.

[10] J. Xiong, R. Ghosh, L. Ma, A. Vaziri, Y. Wang, and L. Wu, "Sandwich-walled cylindrical shells with lightweight metallic lattice truss cores and carbon fiber-reinforced composite face sheets," Compos. Part A Appl. Sci. Manuf., vol. 56, pp. 226-238, Jan. 2014.

[11] T. Zhao et al., "An experimental investigation on low-velocity impact response of a novel corrugated sandwiched composite structure," Compos. Struct., vol. 252, no. June, p. 112676, 2020.

[12] V. Crupi, E. Kara, G. Epasto, E. Guglielmino, and H. Aykul, "Prediction model for the impact response of glass fibre reinforced aluminium foam sandwiches," Int. J. Impact Eng., vol. 77, pp. 97-107, 2015.

[13] R. Mohmmed, F. Zhang, B. Sun, and B. Gu, "Finite element analyses of low-velocity impact failure of foam sandwiched composites with different ply angles face sheets," Mater. Des., vol. 47, pp. 189-199, 2013.

[14] P. B. Su et al., "Axial compressive collapse of ultralight corrugated sandwich cylindrical shells," Mater. Des., vol. 160, pp. 325-337, Dec. 2018.

[15] J. Xiong, A. Vaziri, R. Ghosh, H. Hu, L. Ma, and L. Wu, "Compression behavior and energy absorption of carbon fiber reinforced composite sandwich panels made of three-dimensional honeycomb grid cores," Extreme Mech. Lett., vol. 7, pp. 114-120, 2016.

[16] L. Yan, P. Su, Y. Han, and B. Han, "Effects of Aluminum Foam Filling on Compressive Strength and Energy Absorption of Metallic Y-Shape Cored Sandwich Panel," Metals, vol. 10, no. 12, p. 1670.

[17] H. Fan, L. Yang, F. Sun, and D. Fang, "Compression and bending performances of carbon fiber reinforced lattice-core sandwich composites," Compos. Part A Appl. Sci. Manuf., vol. 52, pp. 118-125, 2013.

[18] Z. Jia Zhang et al., "Mechanical behaviors and failure modes of sandwich cylinders with square honeycomb cores under axial compression," Thin-Walled Struct., vol. 172, p. 108868, Mar. 2022.

[19] Q. Wu et al., "Failure of carbon fiber composite sandwich cylinders with a lattice core under axial compressive loading," Compos. Part A Appl. Sci. Manuf., vol. 155, p. 106812, Apr. 2022.

[20] L. Ge, H. Zheng, H. Li, B. Liu, H. Su, and D. Fang, "Compression behavior of a novel sandwich structure with bi-directional corrugated core," Thin-Walled Struct., vol. 161, p. 107413.

[21] X. Zhu et al., "Experimental study and modeling analysis of planar compression of composite corrugated, lattice and honeycomb sandwich plates," Compos. Struct., vol. 308, p. 116690, Mar. 2023.

[22] X. Zhu et al., "Compression responses of composite corrugated sandwich square tube: Experimental and numerical investigation," Thin-Walled Struct., vol. 169, p. 108440, Dec. 2021.

[23] L. Chen et al., "Compressive response of multi-layered thermoplastic composite corrugated sandwich panels: Modelling and experiments," Compos. B Eng., vol. 189, p. 107899, May 2020.

[24] B. Han, K. Qin, B. Yu, B. Wang, Q. Zhang, and T. J. Lu, "Honeycomb–corrugation hybrid as a novel sandwich core for significantly enhanced compressive performance," Mater. Des., vol. 93, pp. 271-282, Mar. 2016.

[25] H. JO., LS-DYNA Keyword User's Manual Volume II Material Models, Version 971. Livermore Software Technology Corporation, 2017.

[26] S. Murakami, *Continuum failure mechanics: a continuum mechanics approach to the analysis of failure and fracture*.

[27] I. Bozkurt, M. O. Kaman, and M. Albayrak, "Low-velocity impact behaviours of sandwiches manufactured from fully carbon fiber composite for different cell types and compression behaviours for different core types," Mater. Prüfung/Materials Testing, vol. 65, no. 9, pp. 1349-1372, 2023.

[28] P. Feraboli, B. Wade, F. Deleo, M. Rassaian, M. Higgins, and A. Byar, "LS-DYNA MAT54 modeling of the axial crushing of a composite tape sinusoidal specimen," Compos. Part A Appl. Sci. Manuf., vol. 42, no. 11, pp. 1809-1825, Nov. 2011.

[29] F. Dogan, H. Hadavinia, T. Donchev, and P. S. Bhonge, "Delamination of impacted composite structures by cohesive zone interface elements and tiebreak contact," Cent. Eur. J. Eng., vol. 2, no. 4, pp. 612-626, 2012.

[30] I. Bozkurt, M. O. Kaman, and M. Albayrak, "Experimental and numerical impact behavior of fully carbon fiber sandwiches for different core types," J. Braz. Soc. Mech. Sci. Eng., vol. 46, no. 5, p. 318, May 2024.

[31] W. Liu, S. Wang, J. Bu, and X. Ding, "An analytical model for the progressive failure prediction of reinforced thermoplastic pipes under axial compression," Polym. Compos., vol. 42, no. 6, pp. 3011-3024, Jun. 2021.

[32] H. Zhu, P. Wang, D. Wei, J. Si, and Y. Wu, "Energy absorption of diamond lattice cylindrical shells under axial compression loading," Thin-Walled Struct., vol. 181, p. 110131, Dec. 2022.

[33] I. Bozkurt, "Effect of geometric configurations and curvature angle of corrugated sandwich structures on impact behavior," Polym. Compos., pp. 1-24, 2024.

[34] E. Demirci and A. R. Yıldız, "An experimental and numerical investigation of the effects of geometry and spot welds on the crashworthiness of vehicle thin-walled structures," vol. 60, no. 6, pp. 553-561, 2018.

[35] I. Bozkurt, "Numerical Investigation of the Effects of Impactor Geometry on Impact Behavior of Sandwich Structures," Bitlis Eren Univ. J. Sci. Tech., Sep. 2024.

[36] F. Taheri-Behrooz, R. A. Esmaeel, and F. Taheri, "Response of perforated composite tubes subjected to axial compressive loading," Thin-Walled Struct., vol. 50, no. 1, pp. 174-181, Jan. 2012.